Volume 1 | Number 1 | Jan 2013 | Pages 1–100

PCCP

Physical Chemistry Chemical Physics
www.rsc.org/pccp

ROYAL SOCIETY OF CHEMISTRY

ROYAL SOCIETY OF CHEMISTRY

www.rsc.org/pccp

Journal Name

ARTICLE

Non-covalent interactions in water electrolysis: influence on the activity of Pt(111) and iridium oxide catalysts in acidic media

Alberto Ganassin,[a] Viktor Colic,[a] Jakub Tymoczko,[a]

Aliaksandr S. Bandarenka[a,b,*] and Wolfgang Schuhmann[a,*]

Electrolyte components which are typically not considered to be directly involved into catalytic processes at solid-liquid electrified interfaces often demonstrate significant or even drastic influence on the activity, stability and selectivity of electrocatalysts. While there has been certain progress in the understanding of these electrolyte effects, lack of experimental data for various important systems frequently complicates a rational design of new active materials. Modern proton-exchange membrane (PEM) electrolyzers utilize Pt- and Ir-based electrocatalysts which are among the very few materials which are both active and stable under the extreme conditions of water splitting. We use model Pt(111) and Ir-oxide films grown on Ir(111) electrodes and explore the effect of alkali metal cations and sulfate-anions on the hydrogen evolution and the oxygen evolution reactions in acidic media. We demonstrate that sulfate anions decrease the activity of Ir-oxide towards the oxygen evolution reaction while Rb^+ drastically promotes hydrogen evolution reaction at the Pt(111) electrodes as compared to the reference $HClO_4$ electrolytes. Issues related to the activity benchmarking for these catalysts are discussed.

1. Introduction

Water electrolysis is nowadays of particular interest for both fundamental science and energy applications. The former uses hydrogen and oxygen evolution reactions as model processes to improve the understanding of electrified solid/liquid interfaces. On the other hand, hydrogen has been proposed as a promising fuel for sustainable energy provision.[1-5] For these applications energy conversion devices such as proton-exchange membrane (PEM) electrolyzers have been under development for decades.[6-12] They have advantages over other types of electrolyzers, such as a more compact design, higher production rates, and a greater efficiency.[3,13]

The key issue in the electrochemical decomposition of water, particularly using PEM electrolyzers, is that the overall energy losses during the electrocatalytic production of hydrogen largely depend on the choice of the electrode materials. The identification and implementation of new active and stable electrocatalysts is, therefore, of paramount importance for this technology. The state-of-the-art electrocatalyst for the cathodic hydrogen evolution reaction (HER) in acidic media is Pt, being very close to the top of the theoretical activity "volcano" plot.[14] While this reaction is nowadays considered as "less demanding" as compared to the anodic oxygen evolution reaction (OER), still high loadings of Pt are used in PEM electrolyzers (normally between 0.5 and 1 mg/cm^2 [3,15]); and further work to develop more active materials is necessary. In turn, the most active electrocatalysts for OER in acidic media are Ir- and Ru-oxides.[16-18] Ruthenium-based catalysts show the lowest OER overpotential among the oxides, but they suffer from strong corrosion under reaction conditions.[15] Therefore iridium oxides, stable in acidic media at the OER potentials, with slightly lower activity, are known as the state-of-the-art OER catalysts for e.g. PEM electrolyzers.[19]

While the electrode material and its surface structure are considered to be of primary importance to improve the performance of electrolyzers, the resulting electrode activity appeared to be also dependent on the electrolyte composition.[20-26] For instance, hydrogen evolution, particularly in alkaline media, depends on the nature of the alkali metal cations.[20,27] Similarly,

it has been found that the OER activity is significantly influenced by the electrolyte composition in alkaline[28] as well as in acidic sulfuric media.[29] Evidently, the contribution of the electrolyte should be evaluated in each particular case to improve the performance of the PEM electrolyzers and gain further insight into the origin of these effects. Despite certain progress has been made in understanding of the role of the electrolyte composition, many catalytic phenomena at the electrified interface related to the electrolyte side are poorly understood, partly due to a lack of experimental data on model systems.

In this work, we use two model electrodes, namely Pt(111) and iridium oxide thin films grown at the surface of Ir(111) single crystals in order to demonstrate how relevant specific changes in the electrolyte composition influence the electrochemical water splitting. Particularly, we show that species that are not directly involved in the processes, such as sulfate anions for the OER and Rb^+ for the HER, drastically change the activity of the state of the art Pt and iridium oxide electrocatalysts in acidic media. Accordingly, issues related to the activity benchmarking and understanding of these catalytic materials are discussed.

2. Experimental

Experiments were performed in an electrochemical cell described in detail elsewhere.[30,31] Prior to the experiments, all glassware was cleaned with 0.01 M HF solution followed by subsequent multiple rinsing with ultrapure water. HER and OER experiments were performed using Pt(111) and Ir(111) single crystals, respectively, with a sample diameter of 5 mm, surface roughness of 30 nm, and orientation that is better than 0.1° (Mateck, Germany). The preparation and characterization of Pt(111) electrodes prior to each experiment under hanging meniscus configuration was described in detail elsewhere.[30-32] Ir(111) was annealed in the electrochemical cell by means of inductive heating at 1200°C ± 25°C for 10 min under $H_2(10\%)$/Ar flow and cooled in the same atmosphere. The thermal treatment was performed using an inductive heater with an automatic timer controller (20–80 kHz, 15KW - EQ-SP-15A, MTI, USA). A $Hg/HgSO_4$ electrode and a Pt wire (GoodFellow, Germany) were used as reference and counter electrodes, respectively. Working electrolytes were prepared using H_2SO_4 (Merck, Suprapur, Germany), $HClO_4$ (Merck, Suprapur, Germany) and Rb_2SO_4 (99.98%, Sigma Aldrich, Germany), Cs_2SO_4 (99.99%, Sigma Aldrich, Germany), and K_2SO_4 (99.99%, Sigma Aldrich, Germany). All potentials were converted and are referred to the reversible hydrogen electrode (RHE) scale.

The electrodes were immersed into the electrolytes under the potential control at 0.05 V *vs* RHE. The electrochemical response was measured by means of cyclic voltammetry (CV) at a scan rate of 50 mV/s in Ar-saturated solutions (Ar 5.0, Air Liquide, Germany), in oxygen-saturated solution (OER) (O_2 5.0, Air Liquide, Germany) or in hydrogen-saturated solution (HER) (H_2 6.0, Air Liquide, Germany). For HER, and OER measurements, the working electrode was rotated at 1600 rpm and 800 rpm, respectively, using a Gamry RDE 710 rotating disk electrode (RDE) equipment. Electrochemical impedance spectroscopy (EIS) measurements were performed to allow for *iR*-correction. The probing frequencies were varied between 30 kHz and 100 Hz with a 5 mV amplitude of the probing signals for HER, between 3 kHz and 100 Hz with 10 mV probing signal amplitude for OER. Prior to HER and OER experiments, the quality of the Pt(111) and Ir(111) surfaces was assessed via

their characteristic CVs in H_2SO_4 and $HClO_4$ electrolytes. The Ir(111)/oxide surfaces were always freshly prepared starting from the Ir(111) surface followed by the oxidation of the surface in an anodic scan. Anodically formed iridium oxide films (AIROF) were grown via potential cycling between 1.575 V and 0.7 V vs RHE until stable CVs were obtained. This procedure produces stable voltammograms for the OER in the O_2-saturated electrolytes. See schematic presentation of the protocol used in this study in Figure 1.
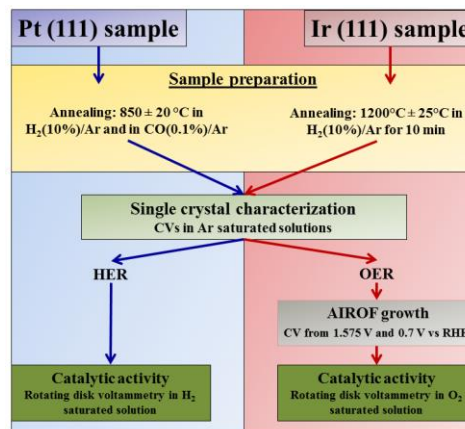
Figure 1. Schematic diagram of the protocol used to investigate non-covalent interactions in HER and OER.

3. Results and Discussion

3.1. Characterization of Pt(111) and Ir(111) single crystal electrodes

To ensure the benchmark quality of the model surfaces, characteristic CVs for Pt(111) (Figure 2A) and Ir(111) (Figure 2B) electrodes in Ar-saturated H_2SO_4 and $HClO_4$ electrolytes were recorded.

For both electrodes, it is possible to judge the quality of the surface and cleanliness of the electrolyte by examining positions and shapes of the voltammetric peaks. For the Pt(111) electrodes, typical well-documented sharp "butterfly" peaks due to either reversible hydroxide adsorption between ~0.6 V and ~0.8 V (in $HClO_4$), or (bi)sulfate adsorption between ~0.35 V and ~0.6 V (in H_2SO_4) can be clearly seen (Figure 1A). Figure 1B, in turn, shows typical CVs recorded for the Ir(111) surface in 0.1 M $HClO_4$ and in 0.1 M H_2SO_4 solutions, facilitating comparison with literature data. Again, the overall shape of the CVs is very close to previously reported ones.[33-37] The characteristic current spikes that can be seen in the region between ~0.05 V and ~0.15 V for H_2SO_4 solutions with the charge involved in the adsorption process of ~240 $\mu C/cm^2$ were documented earlier.[33,34] These spikes likely correspond to a monolayer bonded to the on-top sites of the Ir(111), which is in good agreement with the theoretical value of 252 $\mu C/cm^2$ corresponding to a hydrogen adlayer with a 1:1 ratio of *H to Ir atoms involving a one-electron-transfer reaction at an ideal Ir(111)-(1x1) surface.[33] The current understanding is that during the anodic sweep, sulfates replace some of the hydrogen adatoms and cover the Ir(111) surface until the oxidation process of the Ir(111) starts to occur. STM measurements have shown that sulfates form an ordered √3x√7 structure.[333,37] A reversible *OH adsorption process can be seen in the CV

recorded in 0.1 M $HClO_4$. The larger width of the peak is associated with the *OH adsorption process (a hump if compared to the spike observed in the same solution with Pt(111)) and the absence of symmetry to the potential axis in the CV indicates that the kinetics of the adsorption is slower than on Pt(111).

(A)
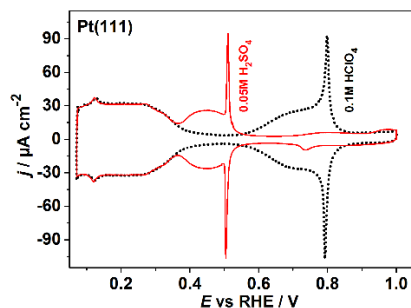
(B)
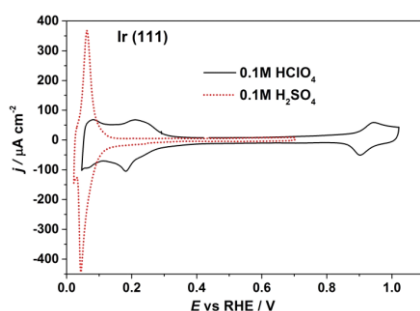
Figure 2. Characteristic CVs in H_2SO_4 and $HClO_4$ electrolytes for (A) Pt(111) and (B) Ir(111) single crystal electrodes. The electrochemical characterization of Pt(111) and Ir(111) single crystal electrodes reveal close to the state-of-the-art surface quality.

3.2. Hydrogen evolution reaction

In an electrolyzer, the activity of metal catalysts for the catho-dic reaction ($2H^+ + 2e^- = H_2$) can in principle be described using a *H-binding adsorption energy descriptor. HER takes place at potentials which are more negative than the potential of zero charge for Pt; therefore, anions are not expected to be specifically adsorbed on the surface. For example, in $HClO_4$ perchlorate anions do not specifically adsorb on the Pt surface in a wide potential window.[38] On the other hand, and as can be seen in Figure 2A, in H_2SO_4 solutions the (bi)sulfate layer is desorbed from the surface at ~0.3 V vs RHE, i.e. well more positive than the potential of the onset of the HER. As can be seen in Figure 3, after iR correction the CVs of the Pt(111) elec-trodes reveal similar HER activity in both H_2-saturated 0.05 M H_2SO_4 and 0.1 M $HClO_4$ electrolytes. Therefore, one can con-clude that the nature of the anions (either sulfate or perchlorate) as well as the ionic strength of the electrolyte do not significantly affect the HER and hydrogen oxidation reaction (HOR) under the given experimental conditions.

In contrast, the presence of cations, such as alkali metal ions, can significantly influence these two reactions as well as the base voltammetry of Pt(111) electrodes. Figure 4 shows charac-teristic CVs of Pt(111) in 0.05 M H_2SO_4, and 0.05 M H_2SO_4 + 0.05 M Me_2SO_4 (Me = K^+, Rb^+, Cs^+), particularly to compare the shape and area of the *H adsorption/desorption region. Ac-cording to physico-chemical properties, the group of alkali metals can be divided into subgroups, where K^+, Rb^+, and Cs^+ belong to the same subgroup. In fact, there are large changes in

atomic and ionic parameters between Na^+ and K^+ and comparably small changes between K^+, Rb^+, and Cs^+.[39,40]

The Pt(111) electrode gives rather symmetrical cyclic voltammograms in K^+, Rb^+, and Cs^+-containing electrolytes, which are however different. The "butterfly" peaks, assigned to the disorder/order phase transition, are shifted towards more positive potentials with increasing atomic weight of the alkali metal cation. An additional check of whether this is caused by surface roughening can be performed afterwards in pure sulfuric acid; it is possible to restore the voltammogram similar to that as shown in Figure 4 for H_2SO_4, suggesting that no significant damages were introduced to the surface. As shown in [27], cations do affect e.g. the HOR in alkaline solutions. In Figure 4, CVs for the case of K_2SO_4 and Rb_2SO_4 show no significant difference in the *H adsorption/desorption region whilst in the case of Cs_2SO_4 there is a slight negative shift in the onset of the *H adsorption/desorption, likely due to adsorption of Cs^+ ions similar to the effect reported earlier.[22]

(A)
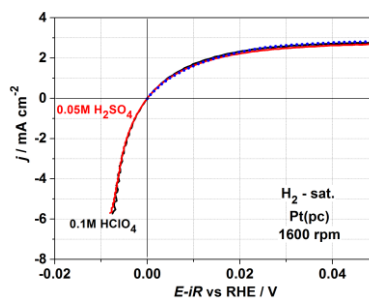
(B)
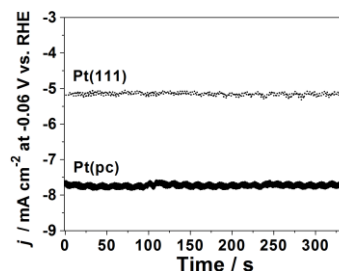
Figure 3. (A) RDE voltammograms of polycrystalline Pt electrodes in H_2 saturated 0.05 M H_2SO_4 and 0.1 M $HClO_4$ electrolytes. Dotted line shows a theoretical curve for the HOR under diffusion control calculated using Nernst equation, similar to ref [41]. (B) Chrono-amperograms taken at -0.06 V, 1600 r.p.m., in H_2 saturated 0.1 M $HClO_4$ comparing the activity of Pt(polycrystalline) and Pt(111) to-wards HER.

As mentioned above, the spikes describing the (bi)sulfate adsorption region are affected by the nature of the cation. According to [42] the positive potential shift with increasing atomic number and concentration of the alkali cation (Me^+) can be attributed to the substitution of H^+ by Me^+ in the hypothetic reaction described by the adsorption equilibrium of $Me^+ + SO_4^{2-} \leftrightarrow Me–SO_4(ad) + 2e^-$ and the concomitant breaking of the hydrogen-bond structure formed between the adsorbates. The shift in the potential peak is accompanied by a decrease of its height due to the breaking of the ordered $\sqrt{3}x\sqrt{7}$ structure. The decrease in the spike height is visible in particular in the case of Rb_2SO_4. It is therefore evident from the CVs in Figure 4 that when the surface is charged negatively with respect to the solution and anions are adsorbed at the surface, alkali metal cations can perturb the adsorbed layer via electrostatic interactions.

However, upon the addition of alkali cations, processes taking place at potentials more negative than the potential of zero charge of Pt(111) can be also affected. One example is shown in Figure 5, in which linear sweep voltammograms in the potential range of HOR and HER reactions in 0.05 M H_2SO_4 + 0.05 M Me_2SO_4, (Me = K^+, Rb^+, Cs^+) are shown. Changes in the HER activities upon the variation of alkali metal cations in solution do not follow the trend of the increasing radii and hydration enthalpies and entropies of the alkali metal cations.[39] At a given current density of e.g. 2 mA/cm², the overpotential increases in the order $Rb^+ > Cs^+ > K^+$. Despite common properties of these cations in the electrolytes, the Rb^+ drastically increases the activity of the Pt(111) electrode.
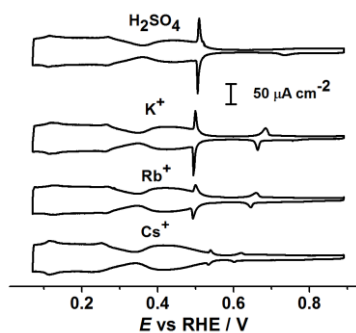
Figure 4. Cyclic voltammogramms at Pt(111) electrodes in Ar-saturated 0.05 M H_2SO_4 and 0.05 M H_2SO_4 + 0.05 M Me_2SO_4, (Me = K^+, Rb^+, Cs^+); scan rate 50 mV/s.
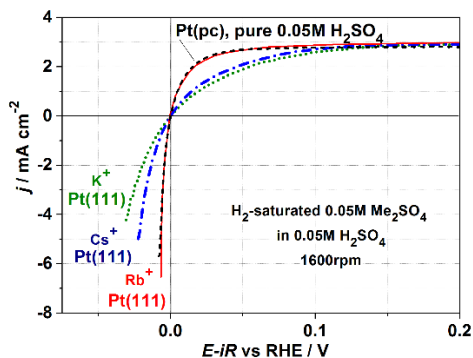
Figure 5. *iR*-corrected RDE-voltammograms characterizing HER/HOR on Pt(111) and polycrystalline Pt in H_2 saturated 0.05 M H_2SO_4 and in 0.05 M H_2SO_4 + 0.05 M Me_2SO_4, (Me = K^+, Rb^+, Cs^+), as indicated in the Figure (scan rate 50 mV/s). See also activities for polycrystalline Pt and Pt(111) and in H_2SO_4 and $HClO_4$ in Figure 1 for comparison.

Surprisingly, it can be noticed that the activity for both HER and HOR in Rb^+ containing electrolyte at a Pt(111) electrode is almost exactly the same as the activity at the polycrystalline Pt electrode. This result suggests that tuning of the electrolyte composition could potentially be as an effective strategy as changing of the electrode surface properties to achieve improved electrocatalytic performance. While further detailed investigations are necessary, we can speculate that non-specifically adsorbed Rb^+ ions cause a destabilization of the quasi-ordered water molecule layer at the surface where H^+ is located in the double layer, thus changing the energy barrier necessary to reduce H^+ to *H. An additional however unlikely contribution to this destabilization could be due to the β^- decay

of the [87]Rb isotope which is always present in natural sources of Rb.

3.3. Oxygen evolution reaction

The effect of the electrolyte composition was also investi-gated for the OER at model Ir-oxide electrodes. Iridium oxide thin films were electrochemically grown on the Ir(111) surface. Anodically formed iridium oxide films (AIROF) were grown by means of potential cycling between 1.575 V and 0.7 V vs RHE until stable CVs were obtained. The lower potential limit was selected to avoid aging, occurring when the oxide film is reduced at negative potentials.[43] The mechanism of the Ir-oxide growth has been investigated in detail before.[44-47] The basis of the widely accepted hypothesis is that anodic oxidation of noble metals is believed to take place on the surface of the non-oxidized iridium electrode via chemisorption of OH radicals and O atoms. According to [48] a monolayer of *OH on the surface of iridium forms at potentials between 1.1 and 1.2 V (SHE) in sulfuric acid solution, whereas a monolayer of *O atoms forms between 1.4 to 1.5 V (SHE).

The effect of the anion on the oxidation process occurring at the Ir(111) surface can be clearly seen in the oxidation peak of the first voltammogram (Figure 6). The sulfate anions at the interface hinder the oxidation of the metallic surface shifting the peak to more positive potentials.
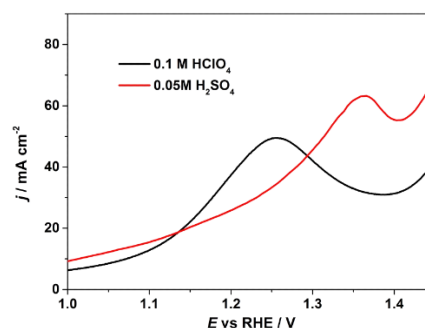
Figure 6. Peak associated with the formation of an oxide monolayer on Ir(111). Scan rate 50 mV/s, O_2-saturated solutions.

One of the characteristic voltammetric features of anodically grown thin films of Ir-oxide is associated with the change in the oxidation state of Ir during the anodic scan. The pre-peaks shown in Figure 7 are associated with the following reaction:[43]

$$(IrO_2 \cdot nH_2O)_5 + 5e^- + 7H_3O^+ + 2(X^-) \leftrightarrow [Ir_5O_3(OH)_7 \cdot 5nH_2O]^{2+}(X^-)_2 + 7H_2O \qquad (1)$$
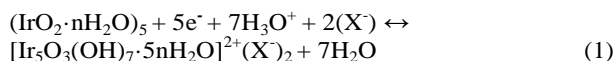
where X^- is the anion present in solution.

Based on electrochemical quartz crystal microbalance (EQCM) measurements the influence of the anion on the stoichiometry of the Ir(III)/Ir(IV) conversion reaction was con-firmed.[47] In this process, both protons and anions are expelled from the oxide during oxidation (and injected during reduction), while the ratio between them is determined by the pH value and the ionic strength. As can be seen in Figure 6 the sulfate anion also influences this process significantly.

Sulfate-anions shift the potential at which the redox transformations occur presumably due to their stronger affinity to the surface. Particularly, the presence of sulfate anions on AIROF has been suggested using results obtained via XPS.[49]

In acidic medium, the following classic simplified reaction scheme (Eqs. 2, 3 and 4) was proposed for the OER on active oxide electrodes:[50]

$$S + H_2O \rightarrow S\text{-}OH_{ads} + H^+ + e^- \qquad (2)$$
$$S\text{-}OH_{ads} \rightarrow S\text{-}O_{ads} + H^+ + e^- \qquad (3)$$
$$2S\text{-}O_{ads} \rightarrow 2S + O_2 \qquad (4)$$

where S is the active site at the oxide surface. Investigations have been carried out on the effect of the pH value in different electrolytes (such as phosphate and sulfate). The pH dependence on the OER exhibited a traditional behavior of 59 mV per pH unit.[51] The effect of different anions in solution on the rate of OER has also been investigated using sulfuric, perchloric, and phosphate solutions on polycrystalline samples.[52] However, since the comparison for the OER has been performed in solutions with effectively different pH values a direct comparison is difficult.

(A)

(B)
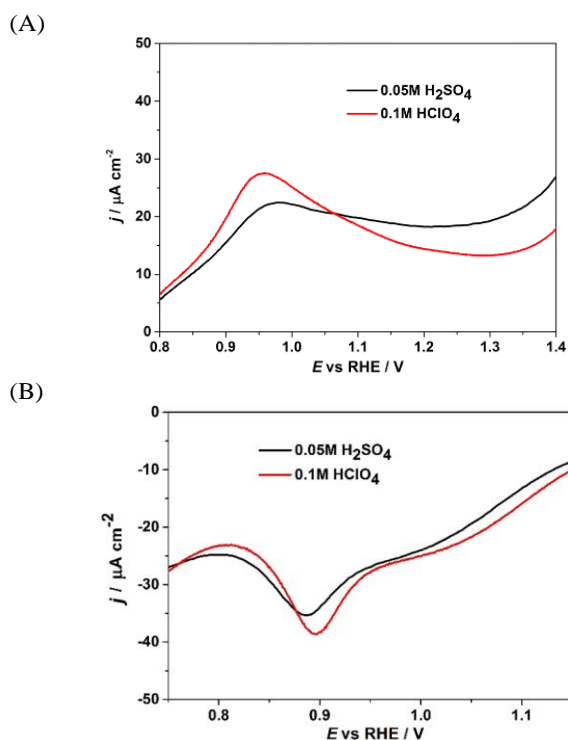
Figure 7. (A) Anodic and (B) cathodic voltammetric peaks associated with the redox transformations according to Eq. 1. Scan rate 50 mV/s, O$_2$-saturated solution.

As can be seen in Figure 8, SO$_4^{2-}$ ions, which are present in the electrolyte, significantly hinder the OER, as expected from the discussion above.

Figure 9 compares the activities obtained in this work and those which are reported as state-of-the-art in the literature and obtained under similar conditions (anodic growth of the oxides) for Ir-oxides. The outcomes are not compared to the literature activities measured extensively using iridium oxide nanoparticles because of the high uncertainty related to the estimation of their real electrochemically active surface area. However, the highest activity obtained for these kinds of samples at lower overpotentials is also indicated in the Figure. As can be seen from Figure 8, the data obtained for the Ir(111)-oxides in perchloric acid reveal their remarkably high OER activity among the most active extended Ir catalytic surfaces.
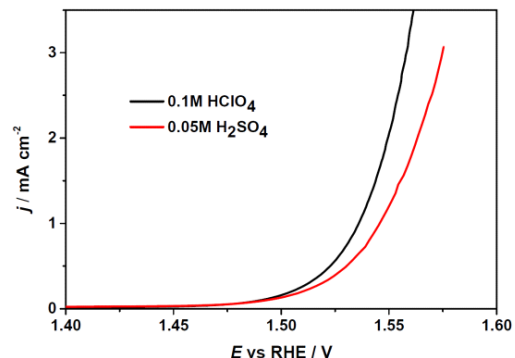
Figure 8. OER activities of Ir-oxide thin films in HClO$_4$ and H$_2$SO$_4$ at pH = 1 (the curves are *iR*-corrected).
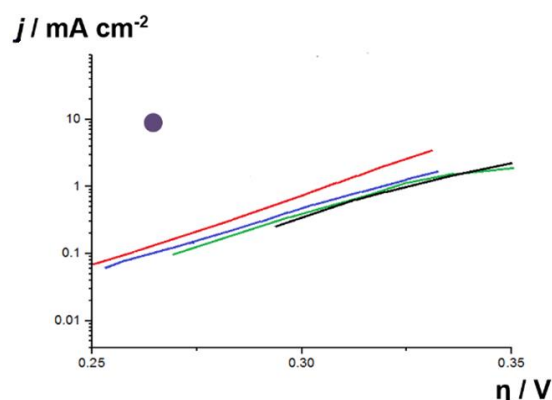
Figure 9. Tafel plots comparing the geometrical current densities vs overpotential for the OER on Ir-oxide films. Green and black lines show data adapted respectively from [53] (OER on AIROF measured in 0.5 M H$_2$SO$_4$) and from [54] (OER on polycrystalline Ir measured in the first scan in deaerated 0.1 M HClO$_4$). Red and blue lines: OER activities measured in this work for AIROF in 0.1 M HClO$_4$ and 0.05 M H$_2$SO$_4$, respectively. The purple spot corresponds to Ir-oxide powders measured in [16] in 1 M H$_2$SO$_4$.

4. Remarks on the electrolyte composition effect on HER and OER

Electrode surface structure and composition as well as electrolyte components contribute to the unique properties of an electrified interface that gives rise to complex metal–ion interactions, which consequently determine the minimal overpotential at which the electrocatalytic reactions can take place. The focus of electrocatalysis nowadays is to find relatively simple relationships describing interactions between the reaction intermediates and the electrode surface, while there is a certain lack of understanding of the influence of the so-called "spectator species". Recent experimental observations, however, suggest that their influence has been often underestimated if not ignored. While there have been indications that it would be possible to describe those interactions with simple descriptors[28,55] such as, for instance, the hydration energy, observations of the catalytic activity of model electrodes in acidic media largely suggest that the situation is perhaps more complex. This situation is somehow similar to the reactions whose trends are understood in alkaline media (e.g. HOR)[27,28] but their understanding in acidic media seems to be much more difficult.[29] Therefore, further extensive experimental and theoretical investigations of model

surfaces to assess the dependence of catalytic properties on the metal/electrolyte interface properties are highly needed. It should be noted that classical heterogeneous catalysis in most of the cases does not experience direct influence of such non-covalent interaction effects. Therefore, identification of the origin of such effects requires efforts from different branches of physico-chemical sciences.

To further underline the particular importance of the electrode/electrolyte interface properties, one can note as a methodological issue that solutions of $HClO_4$ are often used as model electrolytes in electrocatalysis because of their presumably weak interaction with the electrode surface. However, for example, in PEM electrolyzers $HClO_4$ is not the most relevant medium, and the extensive use of Nafion® as proton-conducting membrane arises questions about the influence of sulfonate groups on the efficiency of the system. In fact, the adsorption of sulfates plays an important role concerning the electrocatalytic properties. State-of-the-art catalysts are nearly at the top of the activity volcano plots, and the evaluation of their electrocatalytic properties has to be performed using different solutions, often relevant for practical applications. A different electrolyte composition can in fact mislead the evaluation of reaction kinetics and overpotentials. Further insight into the interaction processes will enable the design of more active nanoparticles, especially taking into account the high cost of Ir and Pt.

In the case of Pt(111) it has been shown that complex interactions of Cl^-, HSO_4^- and SO_4^{2-} anions with the interface and cations present in solution affect the mechanism and kinetics of various reactions.[26,56,57] The effect of the electrolyte on the specific adsorption of the intermediates such as *OH, *O, and *H at Pt in acidic sulfuric media has primary been studied.[58,59] Nonetheless, as it has been shown in this work, the effect of the non-covalent interaction between cations and sulfates on tuning the activity of the Pt have to be considered in the design of electrocatalytic systems with better performance.

5. Summary and conclusions

ClO_4^- and SO_4^{2-} anions are spectators of the HER and HOR on Pt(111) and do not affect the electrocatalytic activity of the catalysts. Perchlorate and (bi)sulfate are not adsorbed in the relevant potential range for the reactions, and the voltammograms for the HOR coincide with the theoretically calculated ones using Nernst equation and assuming diffusion control. Alkali metal cations do influence HER and HOR on Pt(111) surfaces. In particular HER and HOR activities in Rb^+ ions containing electrolytes at a Pt(111) electrode are almost exactly the same as the activity at the polycrystalline Pt electrode.

Perchlorate and sulfate anions have an impact on the oxidation process of Ir(111) and on the OER on AIROF. Specific adsorption of sulfate ions on Ir(111) hinders the oxidation of the metallic surface thus shifting the reaction to more positive potentials. Sulfates also decrease the AIROF activity towards OER if compared to the reaction performed in a solution containing non-specifically adsorbed perchlorate anion.

Acknowledgements

Notes

a Analytical Chemistry - Center for Electrochemical Sciences (CES); Ruhr-Universität Bochum, Universitätsstr. 150, 44780 Bochum; Germany
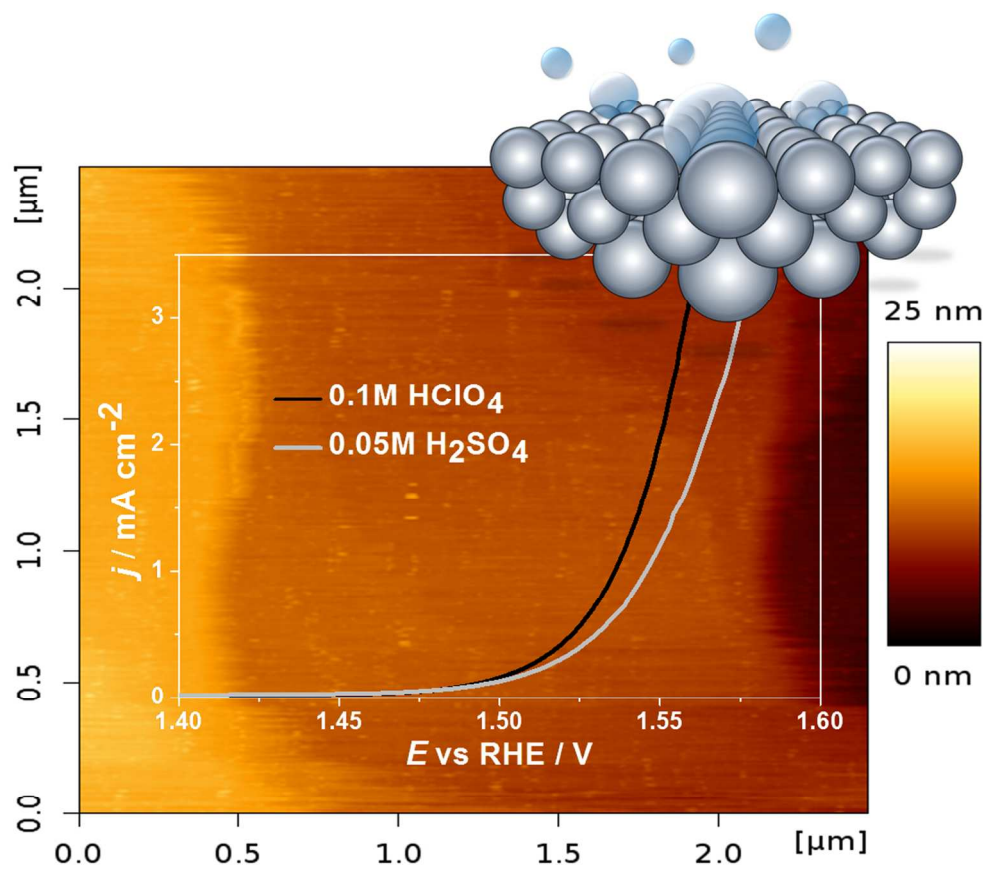b Physik-Department ECS, Technische Universität München, James-Franck-Straße 1, 85748 Garching, Germany

*Corresponding authors, e-mail: bandarenka@ph.tum.de, tel. +49 89 28912531, wolfgang.schuhmann@rub.de, tel. +49 234 3226200

References

1 S. Dutta, *J. Ind. Eng. Chem.*, 2014, **20**, 1148-1156.
2 G. Cipriani, V. Di Dio, F. Genduso, D. La Cascia, R. Liga, R. Miceli and G. R. Galluzzo, *Int. J. Hydrogen Energ.*, 2014, **39**, 8482-8494.
3 M. Carmo, D. L. Fritz, J. Mergel and D. Stolten, *Int. J. Hydrogen Energ.*, 2013, **38**, 490-4934.
4 J. D. Holladay, J. Hu, D. L. King and Y. Wang, *Catal. Today*, 2009, **139**, 244–260.
5 U. Eberle, M. Felderhoff and F. Schüth, *Angew. Chem. Int. Ed.*, 2009, **48**, 6608 – 6630.
6 N. Q. Minh, *J. Am. Ceram. Soc.*, 1995, **76**, 3, 563-588.
7 L. Carrette, K. A. Friedrich and U. Stimming, *ChemPhysChem.*, 2000, **1**, 162-163.
8 F. Babir, *Sol. Energy*, 2005, **78**, 661–669.
9 K. Agbossou, R. Chahine, J. Hamelin, F. Laurencelle, A. Anouar, J. M-St. Arnaud and T. K. Bose, *J. Power Sources*, 2001, **96**, 168-172.
10 D. Shapiro, J. Duffy, M. Kimble and M. Pien, *Sol. Energy*, 2005, **79**, 544–550.
11 H. Iwahara, *Solid State Ionics*, 1988, **28-30**, 573-578.
12 S. H. Jensen, P. H. Larsen and M. Mogensen, *Int. J. Hydrogen Energ.*, 2007, **32**, 3253–3257
13 A. Marshall, B. Børresen, G. Hagen, M. Tsypkin and R. Tunold, *Energ.*, 2007, **32,** 431–436
14 J. K. Nørskov, T. Bligaard, J. Rossmeisl and C. H. Christensen, *Nat. Chem.*, 2009, **1**, 37–46.
15 C. Wannek, W. Lehnert and J. Mergel, *J. Power Sources*, 2009, **192**, 258–266.
16 C. C. L. McCrory, S. Jung, J. C. Peters and T. F. Jaramillo, *J. Am. Chem. Soc.* 2013, **135**, 16977−16987.
17 M. E. G. Lyons and S. Floquet, *Phys. Chem. Chem. Phys.*, 2011, **13**, 5314–5335.
18 T. Reier, M. Oezaslan and P. Strasser, *ACS Catal.* 2012, **2**, 1765−1772.
19 P. Millet, N. Mbemba, S. A. Grigoriev, V. N. Fateev, A. Aukauloo and C. Etievant, *Int. J. Hydrogen Energ.*, 2011, **36**, 4134-4142.
20 N. Danilovic, R. Subbaraman, D. Strmcnik, A. P. Paulikas, D. Myers, V. R. Stamenkovic and N. M. Marković, *Electrocatal.*, 2012, **3**, 221-229.
21 M. Escudero-Escribano, M. E. Michoff, E. P. Leiva, N. M. Marković, C. Gutiérrez and A. Cuesta, *ChemPhysChem.*, 2011, **12**, 2230-2234.
22 B. B. Berkes, G. Inzelt, W. Schuhmann and A. S. Bondarenko, *J. Phys. Chem. C*, 2012, **116**, 10995−11003.
23 M. Nakamura, Y. Nakajima, N. Hoshi, H. Tajiri, O. Sakata, *ChemPhysChem.*, 2013, **14**, 2426 – 2431.

24 D. Strmcnik, D. F. van der Vliet, K.C. Chang, V. Komanicky, K. Kodama, H. You, V. R. Stamenkovic and N. M. Marković, *J. Phys. Chem. Lett.*, 2011, **2**, 2733–2736.

25 G. A. Ragoisha, T. A. Auchynnikava, E. A. Streltsov and S. M. Rabchynski, *Electrochim. Acta*, 2014, **122**, 218–223.

26 C. Stoffelsma, P. Rodriguez, G. Garcia, N. Garcia-Araez, D. Strmcnik, N. M. Marković and M. T. M. Koper, *J. Am. Chem. Soc.*, 2010, **132**, 16127–16133.

27 D. Strmcnik, K. Kodama, D. van der Vliet, J. Greeley, V. R. Stamenkovic and N. M. Marković, *Nat. Chem.*, 2009, **1**, 466-472.

28 J. Suntivich, E. E. Perry, H. A. Gasteiger and Y. Shao-Horn, *Electrocatal.*, 2013, **4,** 49–55.

29 J. Tymoczko, V. Colic, A. Ganassin, W. Schuhmann and A. S. Bandarenka, *Catal. Today*, 2014, 10.1016/j.cattod.2014.07.007.

30 J. Tymoczko, W. Schuhmann, and A. S. Bandarenka, *Phys. Chem. Chem. Phys*. 2013, **15**, 12998-13004.

31 A. S. Bondarenko, I. E. L. Stephens and I. Chorkendorff, *Electrochem. Commun.*, 2012, **23**, 33-36.

32 A. S. Bondarenko, I. E. L. Stephens, H. A. Hansen, F. J. Pérez-Alonso, V. Tripkovic, T. P. Johansson, J. Rossmeisl, J. K. Nørskov and I. Chorkendorff, *Langmuir,* 2011, **27**, 2058-2066.

33 L. J. Wan, M. Hara, J. Inukai and K. Itaya, *J. Phys. Chem. B*, 1999, **103**, 6978-6983.

34 R. Gómez and M. J. Weaver, *Langmuir*, 2002, **18**, 4426-4432.

35 T. Pajkossy, L. A. Kibler and D. M. Kolb, *J. Electroanal. Chem.*, 2005, **582**, 69–75.

36 S. Motoo and N. Furuya, *J. Electroanal. Chem.*, 1984, **181**, 301-311.

37 T. Senna, N. Ikemiya and M. Ito, *J. Electroanal. Chem.* 2001, **511**, 115–121.

38 A. M. Gómez-Marín and J. M. Feliu, *Electrochim. Acta*, 2012, **82**, 558– 569.

39 C. E. Housecroft and A. G. Sharpe, *Inorganic Chemistry*, Pearson Studium, 2006.

40 S. C. Siekierski and J. Burgess, *Concise Chemistry of the Elements*, Woodhead publishing, 2002.

41 W. C. Sheng, H. A. Gasteiger, and Y. Shao-Horn, *J. Electrochem. Soc.*, 2010, **157**, B1529-B1536.

42 G. Cabello, E. P. M. Leiva, C. Gutierrez and A. Cuesta, *Phys. Chem. Chem. Phys.*, 2014, **16**, 14281-14286.

43 H. Elzanowska and V. I. Birss., *J. Appl. Electrochem.*, 1993, **23**, 646–654.

44 P. G. Pickup and V.I. Birss, *J. Electroanal. Chem.*, 1987, **220**, 83-100.

45 J. Juodkazyt, B. Sebeka, G. Stalnionis and K. Juodkazis. *Electroanal.*, 2005, **17**, 1734–1739.

46 V. I. Birss, H. Elzanowska and S. Gottesfeld., *J. Electroanal. Chem.*, 1991, **318**, 327–333.

47 C. Bock and V. I. Birss, *J. Electroanal. Chem.*, 1999, **475**, 20–27.

48 J. Mozota and B. E. Conway, *Electrochim. Acta,* 1983, **28**, 1-8.

49 B. Conway and J. Mozota, *Electrochim. Acta,* 1983, **28**, 9-19.

50 A. J. Bard and M. Stratmann, *Encyclopedia of electrochemistry*, Eds. Wiley-VCH, 2007.

51 L. D. Burke, J. K. Mulcahy and D. P. Whelan*, J. Electroanal. Chem.*, 1984, **163**, 117–128.

52 L. E. Owe, M. Tsypkin and S. Sunde, *Electrochim. Acta*, 2011, **58**, 231–237.

53 M. Vukovic, *J. Appl. Electrochem.,* 1987, **17,** 737–745.

54 T. Reier, M. Oezaslan and P. Strasser, *ACS Catal.,* 2012, **2**, 1765–1772.

55 W. Schmickler and R. Guidelli, *Electrochim. Acta*, 2014, **127**, 489–505.

56 J. X. Wang, N. M. Marković and R. R. Adzic, *J. Phys. Chem. B*, 2004, **108**, 4127−4133.

57 F. El Kadiri, R. Faure and R. Durand, *J. Electroanal. Chem.*, 1991, **301**, 177-188.

58 V. Climent, N. Garcia-Araez and J. M. Feliu, *Electrochem. Commun.*, 2006, **8**, 1577–1582.

59 A. Berna, V. Climent and J. M. Feliu, *Electrochem. Commun.,* 2007, **9**, 2789- 2794.

301x269mm (96 x 96 DPI)